

## Metal–Organic Frameworks

## Polyoxometalate-Encapsulating Cationic Metal–Organic Framework as a Heterogeneous Catalyst for Desulfurization

Xiu-Li Hao,<sup>[a, b]</sup> Yuan-Yuan Ma,<sup>[a]</sup> Hong-Ying Zang,<sup>\*[a]</sup> Yong-Hui Wang,<sup>[a]</sup> Yang-Guang Li,<sup>\*[a]</sup> and En-Bo Wang<sup>[a]</sup>

**Abstract:** A new cationic triazole-based metal–organic framework encapsulating Keggin-type polyoxometalates, with the molecular formula  $[\text{Co}(\text{BBPTZ})_3][\text{HPMo}_{12}\text{O}_{40}] \cdot 24\text{H}_2\text{O}$  [compound **1**; BBPTZ = 4,4'-bis(1,2,4-triazol-1-ylmethyl)bi-phenyl] is hydrothermally synthesized and characterized by elemental analysis, IR spectroscopy, thermogravimetric analysis, powder X-ray diffraction, and single-crystal X-ray diffraction. The structure of compound **1** contains a non-interpen-

etrated 3D  $\text{CdSO}_4$  (cds)-type framework with two types of channels that are interconnected with each other; straight channels that are occupied by the Keggin-type POM anions, and wavelike channels that contain lattice water molecules. The catalytic activity of compound **1** in the oxidative desulfurization reaction indicates that it is not only an effective and size-selective heterogeneous catalyst, but it also exhibits distinct structural stability in the catalytic reaction system.

## Introduction

Metal–organic frameworks (MOFs) have emerged as a class of state-of-the-art materials with designable and multiple functionalities. In this research field, the scope for employment of functional organic linkers in MOFs and the encapsulation of different active entities, such as metal or metal oxide nanoparticles or luminescent, dye, and medicine molecules, within their channels have led to the development of MOFs for a wide variety of uses, such as catalysis, luminescence, molecular detection, or drug delivery.<sup>[1–10]</sup> Introducing polyoxometalates (POMs) into MOF systems to obtain POM-encapsulating MOF (POM@MOF) composite materials is one such hot topic in this field.<sup>[11]</sup> POMs, as a type of nanoscale metal–oxo cluster, have been shown to exhibit activity in acidic, redox, photo-, and electro-induced catalysis. However, POMs' main drawback from the point of view of heterogeneous catalysis is their relatively low specific surface area (SSA).<sup>[12–17]</sup> Therefore, the introduction of such nanoscale molecular catalysts into microporous MOFs brings about the following advantages: i) Improvement of their SSA; ii) uniform dispersal of POM units within a MOF skeleton at the molecular level; iii) affording both POM

units and MOF units with value-added functionalities, such as size-selective catalysis. Additionally, such POM@MOF materials can be easily recycled after catalytic reactions. To synthesize POM@MOF materials, a routine method is direct impregnation of MOFs into POM solution, but this method may not always work well, due to the mismatch between POMs and MOFs in size, charge, structural symmetry, solubility, and pH stability. To date, only a few MOFs, such as MIL-101, HKUST-1 and NENU-11, have been successfully loaded with guest POM catalysts.<sup>[18–20]</sup> Another synthetic strategy is to use POMs as nodes or linkers connecting with metal–organic coordination moieties, to form the POM-based MOFs.<sup>[21,22]</sup> The surface oxygen atoms of POM units in the POM-based MOFs are partially occupied by the metal–organic fragments, which might limit the catalytic properties of the POM units. A third way is to employ POMs as templates, metal ions as nodes, and organic functional groups as linkers to construct POM@MOF hybrid compounds in situ.<sup>[23]</sup> One possible disadvantage of this hybrid material is that the voids of MOFs can be fully occupied by POM units.<sup>[24]</sup> Thus, construction of new POM@MOF hybrid materials while keeping the voids not fully occupied remains a challenge. To be an ideal loading medium for POMs, MOFs should exhibit several properties, as follows: i) MOFs should stably load POMs without loss or framework-collapse during the reaction; ii) POM@MOF materials should retain porous structural features for the entrance and reaction of various substrates; iii) MOFs should be able to improve the loading content of POM catalysts. A promising way to fulfill the above requirements is the construction of cationic MOFs, which can strongly interact with anionic POM units by virtue of electrostatic forces. In this regard, an optimal synthetic route is the use of desired anionic POM catalysts as templates to construct the cationic MOF host in situ with transition metal ions and suitable neutral bridging ligands.

[a] Dr. X.-L. Hao, Y.-Y. Ma, Prof. H.-Y. Zang, Dr. Y.-H. Wang, Prof. Y.-G. Li, Prof. E.-B. Wang  
Key Laboratory of Polyoxometalate Science of Ministry of Education  
Faculty of Chemistry, Northeast Normal University  
Changchun, 130024 (P.R. China)  
E-mail: zanghy100@nenu.edu.cn  
liy658@nenu.edu.cn

[b] Dr. X.-L. Hao  
School of Chemical and Biological Engineering  
Tai Yuan Science and Technology University  
Taiyuan, 030021 (P. R. China)

Supporting information for this article is available on the WWW under <http://dx.doi.org/10.1002/chem.201405825>.

During our investigation of new POM-encapsulating MOF materials, we chose a neutral N-donor semirigid bridging ligand, 4,4'-bis(1,2,4-triazol-1-ylmethyl)biphenyl (BBPTZ). The triazole groups in this ligand usually display strong coordination ability with transition metal ions. Furthermore, the length of BBPTZ ligand is approximately 15.4 Å, which is much longer than the typical Keggin-type POM units (ca. 10 Å; Figure 1). The semirigidity of the ligand endowed the flexibility and elastic ability of pores according to different templates. Therefore,

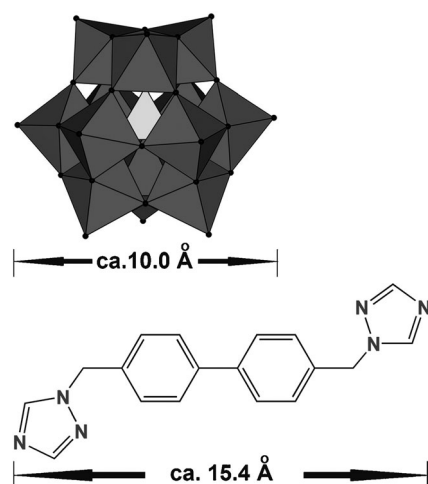


**Figure 1.** Schematic view of the sizes of Keggin-type POM unit (top) and BBPTZ ligand (below).

BBPTZ ligand can be a potential precursor for in situ construction of MOFs encapsulating Keggin-type POM units. Herein, we report a new POM-encapsulating MOF compound,  $[\text{Co}(\text{BBPTZ})_3][\text{HPMo}_{12}\text{O}_{40}] \cdot 24 \text{H}_2\text{O}$  (**1**). Compound **1** contains a cationic 3D  $\text{CdSO}_4(\text{cds})$ -type MOF host with two types of channels that are interconnected with each other; linear channels that are occupied with the Keggin-type POM anions and wavelike channels that are occupied by lattice water molecules. Compound **1** represents the first microporous POM@MOF hybrid compound composed of cationic triazole-based MOF and anionic Keggin-type POM units.<sup>[25]</sup> Oxidative desulfurization is employed as a model catalytic reaction to investigate the catalytic properties of compound **1**, as well as its stability in the organic catalytic reaction system.

## Results and Discussion

### Crystal Structure of **1**

Compound **1** crystallizes in the monoclinic space group  $C2/c$ , and the structural unit contains a cationic 3D MOF motif  $[\text{Co}^{\text{II}}(\text{BBPTZ})_3]^{2+}$ , the  $\alpha$ -Keggin-type polyoxoanion  $[\text{HPMo}_{12}\text{O}_{40}]^{2-}$ , and lattice water molecules. Co ion possessing the +2 oxidation state is confirmed by the X-ray photoelectron spectra (XPS; see the Supporting Information, Figure S5) and the bond valence sum (BVS) calculations (Table S2). In **1**, the cationic MOF possesses one crystallographically independent

$\text{Co}^{2+}$  center (see the Supporting Information, Figure S1). This Co center exhibits a hexacoordinated environment with six nitrogen atoms from the triazole groups of six BBPTZ ligands (Figure S1). The Co–N bond lengths range from 2.136(7) to 2.208(7) Å and the N–Co–N bond angles vary from 87.0(3)° to 180.0(4)°. In this cationic MOF unit, the bridging BBPTZ ligands exhibit two types of configurations, that is, the “U”-type ( $L_U$ ) and “S”-type ( $L_S$ ) configurations (Figure 2a and Figure S2). Each BBPTZ ligand connects with two Co centers. Based on above coordination modes and structural configurations, the Co cen-

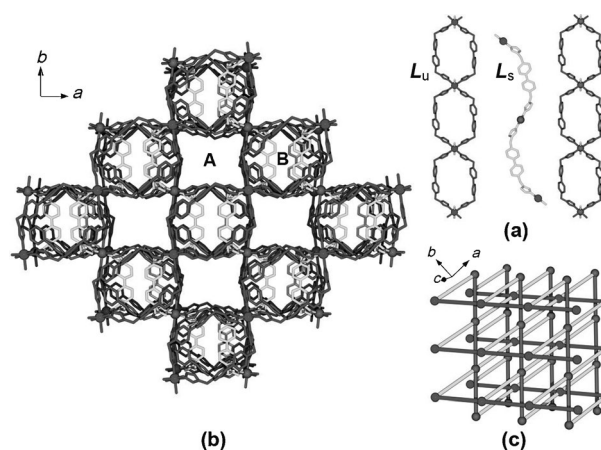


**Figure 2.** a) Ball-and-stick view of the three basic building units in the cationic 3D MOF of **1**; b) the cationic 3D  $\text{cds}$ -type MOF in **1** with two types of channels viewed along  $c$  axis; c) schematic view of the non-interpenetrating  $\text{cds}$ -type framework in **1**.

ters are connected with four  $L_U$  ligands to form 1D loop-containing chains (Figure 2a). These loop-containing chains are parallel to each other on the  $ab$  plane, but the orientations of the chains on two neighboring  $ab$  planes are perpendicular to each other. These loop-containing chains on adjacent  $ab$  planes are further linked together by  $L_S$  ligand via the Co centers, forming a 3D open framework (Figure 2b and Figure S3 in the Supporting Information). From the topological viewpoint, the two parallel BBPTZ ligands in one loop unit can be considered as one linker and the Co centers can be reduced to a four-connected node. Thus, the whole framework adopts the  $\text{CdSO}_4$  ( $\text{cds}$ ) topology, a 4-connected  $\{6^5.8\}$  net (Figure 2c). Most  $\text{cds}$ -type frameworks are interpenetrated due to the self-duality of the  $\text{cds}$  net.<sup>[26,27]</sup> However, compound **1** is a rare example of a  $\text{cds}$ -type framework without an interpenetrating feature. The encapsulation of large polyoxoanions in the  $\text{cds}$ -type net may be an important factor in avoiding interpenetration.

The  $\text{cds}$ -type framework of **1** contains two kinds of channels viewed along  $c$  axis (Figures 2b and 3a). Channel A is straight and filled with the Keggin-type POMs, whereas channel B is undulated and occupied by lattice water molecules (Figure 3b and Figure S4). The window size of channel B is ca. 11.34(1) × 10.87(1) Å. Furthermore, channels A and B are inter-connected with each other, suggesting that the guest molecules in channel B may have the chance to contact with POM units in chan-

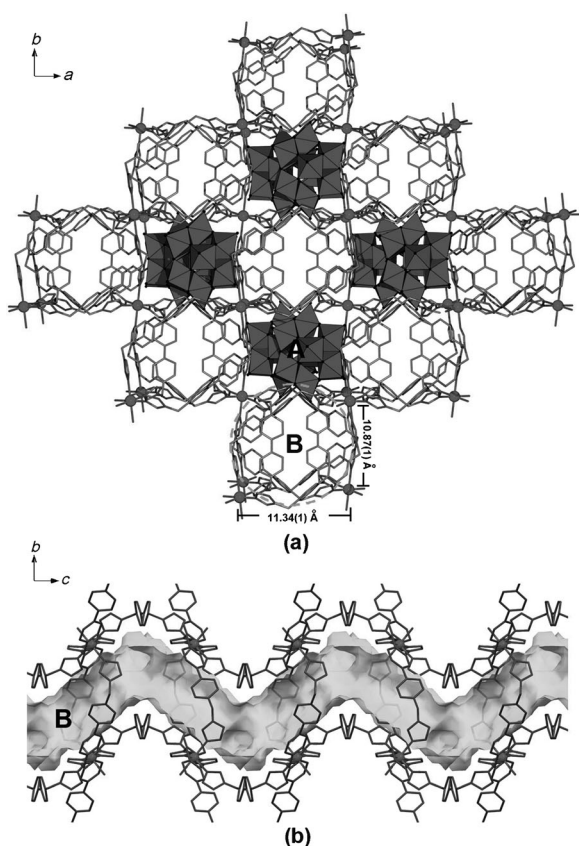


**Figure 3.** a) Ball-and-stick and polyhedral view of the POM@MOF structure of **1** viewed along *c* axis; b) the wavelike channel B in the POM@MOF of **1** viewed along *a* axis. The solvent accessible voids in the channel are modeled with yellow background.

nel A (see the Supporting Information, Figures S3 and S4). Calculations with *PLATON* program<sup>[28]</sup> indicate that the potential solvent area volume is 1929.7 Å<sup>3</sup> after removal of the solvent water molecules, equal to 20.1% of the crystal volume 9586.4 Å<sup>3</sup>. It is worth mentioning that most reported microporous POM@MOF hybrid compounds are based on MOFs constructed by O-donor bridging ligands.<sup>[18–20,23a]</sup> However, compound **1** represents the first microporous POM@MOF composed of cationic triazole-based MOF and anionic Keggin-type POMs. In light of the porous structural of this POM@MOF material, we envisioned that it could be used as a new type of heterogeneous catalyst.

### Catalytic oxidative desulfurization

The desulfurization of fossil fuels is a currently significant task, which is directly associated with the living environment of human beings. In this research field, oxidative desulfurization has been developed as an effective strategy to remove refractory organosulfur substrates, and a key factor in this aspect is the exploration of new oxidative catalyst systems.<sup>[29–32]</sup> Keggin-type polyoxomolybdates have proven effective catalysts for oxidative desulfurization. However, such catalysts are easily soluble in the catalytic reaction system and thus difficult to recycle, which limits their application. The introduction of such POM

catalysts into MOFs is a new route to develop a heterogeneous catalyst system. Herein, the oxidative desulfurization reaction model is used to evaluate the catalytic activity, size selectivity, and stability of compound **1** as a heterogeneous catalyst.

Before the catalytic investigation, the solubility and stability of compound **1** were investigated. Compound **1** was found to be insoluble in various common solvents including water, methanol, ethanol, acetonitrile, and dichloromethane. After immersing compound **1** into the above solvents for 24 h, no signals could be observed from the UV/Vis spectra (see the Supporting Information, Figure S6). The thermogravimetric (TG) analysis curve of compound **1** showed a quite flat stage after all lattice water molecules were removed at 140 °C, suggesting that the framework could be stable after losing the guest water molecules (see the Supporting Information, Figure S7). Based on this experimental result, compound **1** was further treated by heating at 140 °C under vacuum for 8 h. The powder X-ray diffraction (PXRD) pattern of the heat-treated sample of **1** was obtained, which was in agreement with that of untreated compound **1** (Figure 4 and Figure S8 in the Supporting Information). This result further confirmed that the main framework of compound **1** underwent no change after

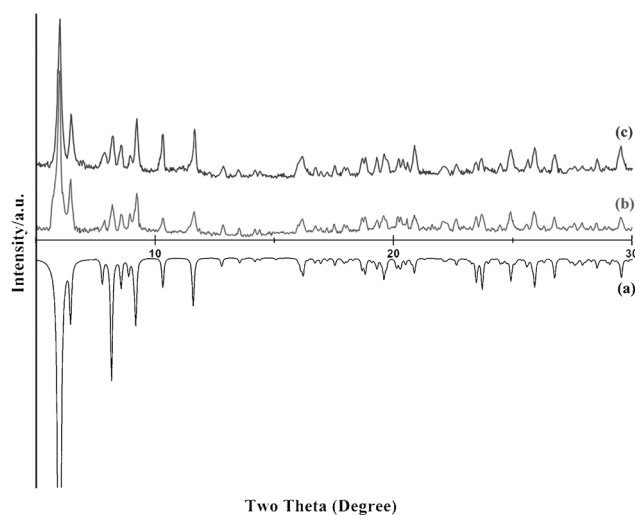
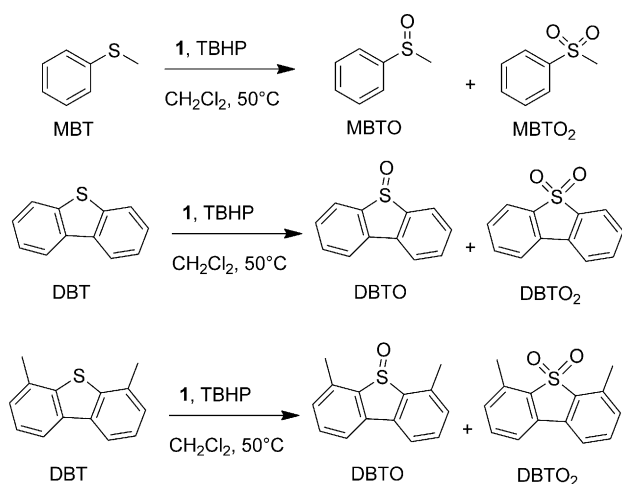


**Figure 4.** PXRD patterns of compound **1** in  $2\theta$  range of 5–30°: a) Simulated pattern; b) as-synthesized sample of **1**; c) heat-treated sample of **1** at 140 °C under vacuum.

removing the lattice water molecules. Moreover, the initial solvent sorption isotherm measurement suggested that heat-treated compound **1** can absorb methanol molecules (see the Supporting Information, Figure S9). Thus, the above heat-treated samples of compound **1** were used as the catalysts for the catalytic reaction.

The catalytic oxidation reaction was performed as follows: Three different sulfide reactants, thioanisole (MBT), dibenzothiophene (DBT), and 4,6-dimethyldibenzothiophene (4,6-DMDBT) reacted with the oxidant *tert*-butyl hydroperoxide (TBHP) in CH<sub>2</sub>Cl<sub>2</sub> medium at 50 °C with compound **1** as the heterogeneous catalyst (Scheme 1).



**Scheme 1.** Oxidation of sulfides thioanisole (MBT), dibenzothiophene (DBT), and 4,6-dimethyldibenzothiophene (4,6-DMDBT) to corresponding sulfoxides and sulfones.

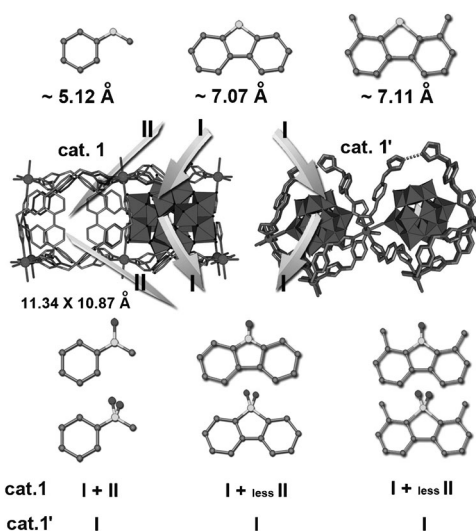
Compound **1** exhibited high catalytic activity for the oxidation of the three sulfide substrates into sulfoxide and sulfone (Table 1). The maximum conversions were 100% for MBT, 99.16% for DBT, and 99.14% for 4,6-DMDBT, respectively (Table 1 and Figure S10a–c in the Supporting Information). The corresponding oxidized sulfoxide and sulfone products were confirmed by FT/IR spectroscopy and GC-MS (see the Supporting Information, Figures S11–S19).

Entry	Sulfide	Product	Catalyst	t	Conversion [%]
1	MBT	MBTO+MBTO <sub>2</sub>	<b>1</b>	15 min	100
2	MBT	MBTO+MBTO <sub>2</sub>	none	300 min	74.04
3	MBT	MBTO+MBTO <sub>2</sub>	<b>1'</b>	50 min	100
4	DBT	DBTO+DBTO <sub>2</sub>	<b>1</b>	8 h	99.16
5	DBT	DBTO+DBTO <sub>2</sub>	<b>1'</b>	9 h	98.1
6	DMDBT	DMDBTO+DMDBTO <sub>2</sub>	<b>1</b>	8 h	99.14
7	DMDBT	DMDBTO+DMDBTO <sub>2</sub>	<b>1'</b>	9 h	98.56

[a] Sulfide (0.4 mmol), TBHP (1.5 mmol) and catalyst (10.0 mg) were mixed in CH<sub>2</sub>Cl<sub>2</sub> (5 mL) at 50 °C with continuous stirring. The conversion was obtained by HPLC analysis with a UV/Vis detector at λ = 254 nm using an Inertsil SIL-100A C18 column.

As control experiments, oxidation of MBT was also performed with a mixture of Co(OAc)<sub>2</sub> and BBPTZ and without any catalyst, which gave conversions of 77.13% and 74.04% from MBT to MBTO/MBTO<sub>2</sub> in 300 min, respectively (Table 1 and Figure S10g,h in the Supporting Information). The results indicate that compound **1** is a potentially effective catalyst in the oxidative desulfurization process and that the main catalytic center is the POM unit. Furthermore, another POM-templated organic–inorganic hybrid compound, **1'**, with the chemical formula [Co<sup>II</sup>(HBBTZ)(BBTZ)<sub>2.5</sub>][PMo<sub>12</sub>O<sub>40</sub>] (BBTZ = 4,4'-bis(1,2,4-triazol-1-ylmethyl)benzene)<sup>[24b]</sup> was used as a reference catalyst for the oxidation of MBT. Compound **1'** has the similar chemi-

cal composition to compound **1** but incorporates no solvent-accessible voids in its hybrid crystal structure (see the Supporting Information, Figure S20). The catalytic oxidation of MBT into MBTO/MBTO<sub>2</sub> with compound **1'** achieved a conversion of 100% in 50 min, which was obviously slower than the reaction catalyzed by compound **1** (Table 1 and Figure S10d in the Supporting Information). Such a difference suggests that the catalytic oxidative desulfurization may just happen on the surface of compound **1'** and only POMs on the surface of the framework play a catalytic role in the reaction. However, the porosity of compound **1** may lead to the POM units both on the surface and within the voids acting as catalytic sites, which may accelerate the oxidation reaction (Scheme 2).



**Scheme 2.** Different catalytic reaction routes among the sulfide substrates and different catalysts, based on the catalytic results. Route I represents catalysis taking place on the surface of catalysts; Route II represents catalysis taking place within the channels of catalysts.

The oxidative desulfurization of DBT and DMDBT into relevant sulfoxide and sulfone products with compounds **1** and **1'** were also investigated. The catalytic oxidation of DBT and DMDBT achieved conversion of approximately 99% in 8 h with **1** and approximately 98% in 9 h with **1'** (Table 1 and Figure S10b,c,e,f in the Supporting Information). These experimental results suggest that compounds **1** and **1'** possess quite similar catalytic activities for the oxidative desulfurization of DBT and DMDBT. In one regard, such slow oxidation processes are probably due to the relatively strong antioxidant property of DBT and DMDBT substrates. However, it is more possible that the catalytic oxidation of DBT and DMDBT by both **1** and **1'** mainly happens on the surface of these catalysts. Especially considering the larger sizes of DBT and DMDBT molecules than MBT molecules, DBT and DMDBT may not easily fit through the wavelike channels of compound **1** (Scheme 2). In contrast to other well-known POM@MOF- or POM-based porous materials used for catalytic oxidative desulfurization,<sup>[19c,30]</sup> compound **1** displays relatively low catalytic activities in the oxidation of DBT and DMDBT due to the smaller pore size of compound **1**

than those of the previously reported composites.<sup>[19c,30]</sup> Thus, the pore size and volume of MOF units should be another important factor for the catalytic activity of POM@MOF composites.

The effect of the size of catalyst particles on the catalytic activity was also checked. When a sample of **1** with an average particle size of 300  $\mu\text{m}$  was used in the oxidation of MBT, the conversion was 98.56% in 15 min. Under the same conditions, a ground sample of **1** with an average particle size of 40  $\mu\text{m}$  gave a conversion of 100% in 15 min (see the Supporting Information, Figure S21). This result suggests that the size of catalytic sample **1** has no obvious influence on the catalytic activity.

Compound **1** is insoluble in the reaction system and can be easily recycled by simple centrifugal separation (see the Supporting Information, Figure S22). Notably, no obvious changes were observed in the FT/IR spectra, UV/Vis diffuse reflectance spectra, or powder X-ray diffraction (PXRD) data of compound **1** before and after six catalytic cycles (see the Supporting Information, Figures S23–S25), suggesting that the porous framework of compound **1** is stable in this catalytic reaction system. Furthermore, the catalytic lifetime of compound **1** was tested. The recycled catalyst was reused for six cycles and the conversion was only slightly decreased, suggesting that the catalytic activity of compound **1** can be well maintained (see the Supporting Information, Figure S26).

## Conclusion

In summary, a new POM@MOF compound was synthesized, consisting of a cationic triazole-based MOF encapsulating POM anions. The heterogeneous catalytic property of the POM@MOF compound was investigated by using the oxidative desulfurization reaction model, indicating that compound **1** not only exhibited effective catalytic activity and size-selective properties, but also showed distinct structural stability. Furthermore, compound **1** was easily recycled by simple centrifugal separation. Compound **1** represents a new POM@MOF hybrid example, which is composed of a cationic porous MOF based on N-donor ligands and Keggin-type polyoxoanions. Moreover, the catalytic activities of such POM@MOF composites are not only dependent on the POM moieties but also the pore size and volume of the MOF units. Therefore, more POM@MOF compounds based on Keggin-type POM units with different components and various in situ-assembled cationic triazole-based MOF systems with larger pore sizes and volumes could be explored, so as to obtain new catalytically active POM@MOF compounds. This work is ongoing in our group.

## Experimental Section

### Materials and Methods

All chemicals and organic solvents used for synthesis were of reagent grade without further purification. The ligand 4,4'-bis(1,2,4-triazol-1-ylmethyl)biphenyl (BBPTZ) was synthesized according to the literature.<sup>[33]</sup>  $\text{H}_3\text{PMo}_{12}\text{O}_{40}\cdot n\text{H}_2\text{O}$  was prepared according to the

reported methods.<sup>[34]</sup> Elemental analyses (C, H, N) were performed on a PerkinElmer 2400 CHN elemental analyzer. The FT-IR spectra were analyzed on a Mattson Alpha-Centauri spectrometer with KBr pellets in the range of 4000–400  $\text{cm}^{-1}$ . TG analyses were carried out on a Pyris Diamond TG instrument in flowing  $\text{N}_2$  with a heating rate of 10  $^\circ\text{C}\cdot\text{min}^{-1}$ . The powder X-ray diffraction (PXRD) studies were performed with a Rigaku D/max-IIIB X-ray diffractometer at a scanning rate of 1  $^\circ$  per minute with  $2\theta$  ranging from 5  $^\circ$  to 50  $^\circ$ , using  $\text{Cu}_{\text{K}\alpha}$  radiation ( $\lambda = 1.5418 \text{ \AA}$ ).

### Synthesis

$[\text{Co}(\text{BBPTZ})_3][\text{HPMo}_{12}\text{O}_{40}]\cdot 24\text{H}_2\text{O}$  (**1**):  $\text{H}_3\text{PMo}_{12}\text{O}_{40}\cdot 24\text{H}_2\text{O}$  (0.6 g, ca. 0.3 mmol),  $\text{Co}(\text{OAc})_2\cdot 4\text{H}_2\text{O}$  (0.087 g, 0.35 mmol), and BBPTZ (0.16 g, 0.5 mmol) were mixed in distilled water (10 mL) and stirred at room temperature for 0.5 h. During this period, the reaction mixture was adjusted to pH 2.0 with 1.0 M NaOH. Then, the suspension was sealed into a Teflon-lined autoclave, kept under autogenous pressure at 130  $^\circ\text{C}$  for 3 days, and then slowly cooled to room temperature. Orange block crystals of **1** were isolated, collected by filtration, washed with distilled water, and kept in a vacuum desiccator (50% yield based on Mo). Selected IR (KBr pellet):  $\tilde{\nu} = 3446(\text{w})$ , 3113(m), 3030(w), 1612(m), 1522(s), 1438(m), 1403(w), 1346(w), 1281(s), 1210(m), 1132(s), 1057(s), 1010(w), 956(s), 879(w), 802  $\text{cm}^{-1}$  (s); elemental analysis calcd (%) for  $\text{C}_{54}\text{H}_{97}\text{N}_{18}\text{O}_{64}\text{PMo}_{12}\text{Co}$ : C 19.85, H 2.97, N 7.72; found: C 19.88, H 2.95, N 7.70. TG curve suggests that compound **1** contains approximately 24 lattice water molecules (see the Supporting Information, Figure S6).

### X-ray Crystallography

Single-crystal X-ray diffraction data for compound **1** was collected at 150(2) K on the Bruker Apex CCD diffractometer using graphite monochromatic  $\text{Mo}_{\text{K}\alpha}$  radiation ( $\lambda = 0.71073 \text{ \AA}$ ). A multi-scan absorption correction was applied. The structure was solved by the direct method and refined by a full-matrix least-squares method on  $F^2$  using the SHELX-97 crystallographic software package.<sup>[35,36]</sup> During the refinement of **1**, non-hydrogen atoms were refined anisotropically except the lattice water molecules. During the anisotropic refinement, some C atoms on the organic ligands possess the anisotropic displacement parameters (ADP) problem. Thus, the restrained command 'ISOR' was used to restrain such atoms so as to avoid the ADP problems. Furthermore, the five-membered triazole rings and the six-membered benzene rings in the organic ligands are structurally unreasonable, thus, the restrained command 'AFIX 59/AFIX 0', 'AFIX 69/AFIX 0' and 'DELU' were used to fix these five- and six-membered rings with reasonable structural features. All above restrained refinement led to a restrained value of 102. The H atoms on organic C centers were fixed in calculated positions. H atoms on water molecules cannot be assigned from the weak reflection peaks but directly included into the final molecular formula. In the final refinement, only two lattice water molecules can be assigned from the weak residual peaks. However, the structural feature suggests that there are still solvent-accessible voids in the compound. Thus, the SQUEEZE program was further used to remove the contributions of weak reflection for the crystal data and a new calculation result 1\*.hkl was further used to refine the whole crystal structure.<sup>[28]</sup> Based on the SQUEEZE calculation results, elemental analysis, and TG analysis, another twenty two lattice water molecules were directly added in the final molecular formula of compound **1**. Crystal data and structure refinement for compound **1** is listed in Table 2. Selected bond lengths and angles of **1** are listed in Table S1 in the Supporting Information.

**Table 2.** Crystal data and structure refinement for 1.

Formula	C <sub>54</sub> H <sub>97</sub> N <sub>18</sub> O <sub>64</sub> PMo <sub>12</sub> Co
M <sub>r</sub>	3263.68
T [K]	150(2)
Cryst. Syst.	Monoclinic
Space group	C2/c
a [Å]	20.429(2)
b [Å]	22.744(2)
c [Å]	21.792(2)
α [°]	90
β [°]	108.783(2)
γ [°]	90
V [Å <sup>3</sup> ]	9586.4(2)
Z	4
μ [mm <sup>-1</sup> ]	1.817
F(000)	6420
Reflections	27 790
R <sub>int</sub>	0.0672
GOF	1.022
R <sub>1</sub> [I > 2σ(I)] <sup>[a]</sup>	0.0702
wR <sub>2</sub> (all data) <sup>[b]</sup>	0.2086

[a]  $R_1 = \frac{\sum ||F_o| - |F_c||}{\sum |F_o|}$ ; [b]  $wR_2 = \frac{\sum [w(F_o^2 - F_c^2)^2]}{\sum [w(F_o^2)^2]}^{1/2}$ .

CCDC 964639 (1) contains the supplementary crystallographic data for this paper. These data can be obtained free of charge from the Cambridge Crystallographic Data Centre via [www.ccdc.cam.ac.uk/data\\_request/cif](http://www.ccdc.cam.ac.uk/data_request/cif).

### Oxidative desulfurization

The oxidative desulfurization reaction model was performed with three kinds of sulfides, that is, thioanisole (MBT), dibenzothiophene (DBT), and 4,6-dimethyl dibenzothiophene (4,6-DMDBT). In a typical case, sulfide (0.4 mmol) and *tert*-butyl hydroperoxide (TBHP; 1.5 mmol, 1.35 mg) were dissolved in CH<sub>2</sub>Cl<sub>2</sub> (5 mL). Then compound 1 (0.05 mmol) was added into the above solution as the heterogeneous catalyst, and the catalytic reaction was performed at 50 °C with continuous stirring. An aliquot (150 μL) of the reaction mixture was periodically removed and put into an ice chamber to stop the reaction. The catalytic products were determined by FT/IR and GC-MS, and the reaction yields were obtained by HPLC analysis with a UV/Vis detector at λ = 254 nm using a Inertsil SIL-100 A C18 column. All analyses were performed with the mobile phase: CH<sub>3</sub>CN/H<sub>2</sub>O = 90:10 at an operating flow rate of 1 mL min<sup>-1</sup>.

### Acknowledgements

This work was supported by National Natural Science Foundation of China (grant nos. 21271039, 21201032 and 21471028), Program for New Century Excellent Talents in University (grant no. NCET120813) and Fundamental Research Funds for the Central Universities (grant no. 11SSXT140).

**Keywords:** cobalt • heterogeneous catalysis • metal-organic frameworks • oxidative desulfurization • polyoxometalates

- [1] a) M. Li, D. Li, M. O'Keefe, O. M. Yaghi, *Chem. Rev.* **2014**, *114*, 1343–1370; b) W. G. Lu, Z. W. Wei, Z. Y. Gu, T. F. Liu, J. Park, J. Tian, M. W. Zhang, Q. Zhang, T. Gentle III, M. Bosch, H. C. Zhou, *Chem. Soc. Rev.*

- 2014**, *43*, 5561–5593; c) Y. B. He, W. Zhou, G. D. Qian, B. L. Chen, *Chem. Soc. Rev.* **2014**, *43*, 5657–5678; d) J. P. Zhang, P. Q. Liao, H. L. Zhou, R. B. Lin, X. M. Chen, *Chem. Soc. Rev.* **2014**, *43*, 5789–5814; e) M. Pan, X. M. Lin, G. B. Li, C. Y. Su, *Coord. Chem. Rev.* **2011**, *255*, 1921–1936.
- [2] A. Ajjaz, T. Akita, N. Tsumori, Q. Xu, *J. Am. Chem. Soc.* **2013**, *135*, 16356–16359.
- [3] C. Y. Sun, X. L. Wang, X. Zhang, C. Qin, P. Li, Z. M. Su, D. X. Zhu, G. G. Shan, K. Z. Shao, H. Wu, J. Li, *Nat. Commun.* **2013**, *4*, 2717.
- [4] Y. Yuan, F. X. Sun, L. N. Li, P. Cui, G. S. Zhu, *Nat. Commun.* **2014**, *5*, 4260.
- [5] K. Manna, T. Zhang, W. B. Lin, *J. Am. Chem. Soc.* **2014**, *136*, 6566–6569.
- [6] C. Y. Sun, C. Qin, C. G. Wang, Z. M. Su, S. Wang, X. L. Wang, G. S. Yang, K. Z. Shao, Y. Q. Lan, E. B. Wang, *Adv. Mater.* **2011**, *23*, 5629–5632.
- [7] M. J. Dong, M. Zhao, S. Ou, C. Zou, C. D. Wu, *Angew. Chem. Int. Ed.* **2014**, *53*, 1575–1579.
- [8] K. Mo, Y. H. Yang, Y. Cui, *J. Am. Chem. Soc.* **2014**, *136*, 1746–1749.
- [9] D. Tian, Q. Chen, Y. Li, Y. H. Zhang, Z. Chang, X. H. Bu, *Angew. Chem. Int. Ed.* **2014**, *53*, 837–841.
- [10] W. W. Zhan, Q. Kuang, J. Z. Zhou, X. J. Kong, Z. X. Xie, L. S. Zheng, *J. Am. Chem. Soc.* **2013**, *135*, 1926–1933.
- [11] D. Y. Du, J. S. Qin, S. L. Li, Z. M. Su, Y. Q. Lan, *Chem. Soc. Rev.* **2014**, *43*, 4615–4632.
- [12] M. T. Pope, *Heteropoly and Isopoly Oxometalates*, Springer-Verlag, Berlin, **1983**.
- [13] a) I. V. Kozhevnikov, *Chem. Rev.* **1998**, *98*, 171–198; b) M. Sadakane, E. Steckhan, *Chem. Rev.* **1998**, *98*, 219–237.
- [14] H. N. Miras, J. Yan, D. L. Long, L. Cronin, *Chem. Soc. Rev.* **2012**, *41*, 7403–7430.
- [15] A. Rubinstein, P. Jiménez-Lozano, J. J. Carbó, J. M. Poblet, R. Neumann, *J. Am. Chem. Soc.* **2014**, *136*, 10941–10948.
- [16] H. J. Lv, J. Song, Y. V. Geletii, J. W. Vickers, J. M. Sumliner, D. G. Musaev, P. Kögerler, P. F. Zhuk, J. Bacsá, G. Zhu, C. L. Hill, *J. Am. Chem. Soc.* **2014**, *136*, 9268–9271.
- [17] X. B. Han, Z. M. Zhang, T. Zhang, Y. G. Li, W. B. Lin, W. S. You, Z. M. Su, E. B. Wang, *J. Am. Chem. Soc.* **2014**, *136*, 5359–5366.
- [18] a) G. Férey, C. Mellot-Draznieks, C. Serre, F. Millange, J. Dutour, S. Surblé, I. Margiolaki, *Science* **2005**, *309*, 2040–2042; b) L. Bromberg, X. Su, T. Alan Hatton, *ACS Appl. Mater. Interfaces* **2013**, *5*, 5468–5477.
- [19] a) C. Y. Sun, S. X. Liu, D. D. Liang, K. Z. Shao, Y. H. Ren, Z. M. Su, *J. Am. Chem. Soc.* **2009**, *131*, 1883–1888; b) J. Song, Z. Luo, D. K. Britt, H. Furukawa, O. M. Yaghi, K. I. Hardcastle, C. L. Hill, *J. Am. Chem. Soc.* **2011**, *133*, 16839–16846; c) Y. W. Liu, S. M. Liu, S. X. Liu, D. D. Liang, S. J. Li, Q. Tang, X. Q. Wang, J. Miao, Z. Shi, Z. P. Zheng, *ChemCatChem* **2013**, *5*, 3086–3091.
- [20] F. J. Ma, S. X. Liu, C. Y. Sun, D. D. Liang, G. J. Ren, F. Wei, Y. G. Chen, Z. M. Su, *J. Am. Chem. Soc.* **2011**, *133*, 4178–4181.
- [21] B. Nohra, H. E. Moll, L. M. R. Albelo, P. Mialane, J. Marrot, C. Mellot-Draznieks, M. O'Keefe, R. N. Biboum, J. Lemaire, B. Keita, L. Nadjo, A. Dolbecq, *J. Am. Chem. Soc.* **2011**, *133*, 13363–13374.
- [22] a) H. Fu, C. Qin, Y. Lu, Z. M. Zhang, Y. G. Li, Z. M. Su, W. L. Li, E. B. Wang, *Angew. Chem.* **2012**, *124*, 8109–8113; *Angew. Chem. Int. Ed.* **2012**, *51*, 7985–7989; b) C. Zou, Z. J. Zhang, X. Xu, Q. Gong, J. Li, C. D. Wu, *J. Am. Chem. Soc.* **2012**, *134*, 87–90.
- [23] a) M. L. Wei, C. He, W. J. Hua, C. Y. Duan, S. H. Li, Q. J. Meng, *J. Am. Chem. Soc.* **2006**, *128*, 13318–13319; b) P. Y. Wu, C. He, J. Wang, X. J. Peng, X. Z. Li, Y. L. An, C. Y. Duan, *J. Am. Chem. Soc.* **2012**, *134*, 14991–14999.
- [24] a) X. L. Hao, Y. Y. Ma, C. Zhang, Q. Wang, X. Cheng, Y. H. Wang, Y. G. Li, E. B. Wang, *CrystEngComm* **2012**, *14*, 6573–6580; b) X. L. Hao, Y. Y. Ma, Y. H. Wang, L. Y. Xu, F. C. Liu, M. M. Zhang, Y. G. Li, *Chem. Asian J.* **2014**, *9*, 819–829.
- [25] a) X. L. Wang, C. Qin, E. B. Wang, Z. M. Su, *Chem. Commun.* **2007**, 4245–4247; b) H. J. Pang, J. Peng, C. J. Zhang, Y. G. Li, P. P. Zhang, H. Y. Ma, Z. M. Su, *Chem. Commun.* **2010**, 46, 5097–5099.
- [26] Most **cds**-type frameworks are interpenetrated, for example: a) O. Delgado-Friedrichs, M. O'Keefe, O. M. Yaghi, *Solid State Sci.* **2003**, *5*, 73–78; b) Q. X. Yang, X. Q. Chen, J. H. Cui, J. S. Hu, M. D. Zhang, L. Qin, G. F. Wang, Q. Y. Lu, H. G. Zheng, *Cryst. Growth Des.* **2012**, *12*, 4072–4082; c) N. F. Zheng, J. Zhang, X. H. Bu, P. Y. Feng, *Cryst. Growth Des.* **2007**, *7*, 2576–2581.

- [27] For examples of non-interpenetrated **cds**-type frameworks see ref. [26b] and: L. D. DeVries, P. M. Barron, E. P. Hurley, C. H. Hu, W. Choe, *J. Am. Chem. Soc.* **2011**, *133*, 14848–14851.
- [28] A. L. Spek, *PLATON, A Multipurpose Crystallographic Tool*, Utrecht University, Utrecht, The Netherlands, **1998**.
- [29] N. Mizuno, K. Kamata, K. Yamaguchi, *Catal. Today* **2012**, *185*, 157–161.
- [30] D. Liu, Y. Lu, H. Q. Tan, W. L. Chen, Z. M. Zhang, Y. G. Li, E. B. Wang, *Chem. Commun.* **2013**, *49*, 3673–3675.
- [31] Z. X. Zhang, F. W. Zhang, Q. Q. Zhu, W. Zhao, B. C. Ma, Y. Ding, *J. Colloid Interface Sci.* **2011**, *360*, 189–194.
- [32] H. Y. Lü, Y. N. Zhang, Z. X. Jiang, C. Li, *Green Chem.* **2010**, *12*, 1954–1958.
- [33] X. R. Meng, Y. L. Song, H. W. Hou, H. Y. Han, B. Xiao, Y. T. Fan, Y. Zhu, *Inorg. Chem.* **2004**, *43*, 3528–3536.
- [34] C. Rocchiccioli-Deltcheff, M. Fournier, R. Franck, R. Thouvenot, *Inorg. Chem.* **1983**, *22*, 207–216.
- [35] G. M. Sheldrick, SHELXS97, Program for Crystal Structure Solution, University of Göttingen, Göttingen, Germany, **1997**.
- [36] G. M. Sheldrick, SHELXL97, Program for Crystal Structure Refinement, University of Göttingen, Göttingen, Germany, **1997**.

---

Received: October 27, 2014  
Published online on ■ ■ ■ ■, 0000

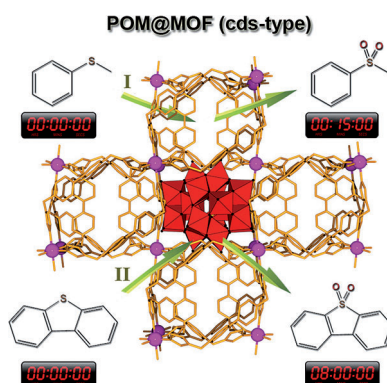
## FULL PAPER

### Metal–Organic Frameworks

X.-L. Hao, Y.-Y. Ma, H.-Y. Zang,\*  
Y.-H. Wang, Y.-G. Li,\* E.-B. Wang



### Polyoxometalate-Encapsulating Cationic Metal–Organic Framework as a Heterogeneous Catalyst for Desulfurization



**Sulfur no more:** A cationic triazole-based metal–organic framework encapsulating Keggin-type polyoxometalates, with the molecular formula  $[\text{Co}(\text{BBPTZ})_3][\text{HPMo}_{12}\text{O}_{40}] \cdot 24 \text{H}_2\text{O}$  [BBPTZ = 4,4'-bis(1,2,4-triazol-1-ylmethyl)biphenyl], is synthesized, characterized and shown to be active in oxidative desulfurization catalysis.